16623-6005-R0-00

INVESTIGATION OF HIGH-SPEED PHENOMENA

FINAL REPORT

by

D. G. Becker and J. C. Slattery

Prepared for
NATIONAL AERONAUTICS AND SPACE ADMINISTRATION
Headquarters
Contract No. NASw-2246

December 1972

TRW
SYSTEMS GROUP

ONE SPACE PARK • REDONDO BEACH, CALIFORNIA 90278

16623-6005-RO-00

INVESTIGATION OF HIGH-SPEED PHENOMENA

FINAL REPORT

by

D.G. Becker and J. C. Slattery

Prepared for

NATIONAL AERONAUTICS AND SPACE ADMINISTRATION
Headquarters

Washington, D.C. 20546

Contract No. NASw-2246

December 1972

TRW SYSTEMS GROUP
One Space Park, Redondo Bech, California

16623-6005-RO-00

INVESTIGATION OF HIGH-SPEED PHENOMENA

FINAL REPORT

December 1972

Prepared by _____
D. G. Becker
Member of the Professional Staff
Systems Group Research Staff

and _____
J. C. Slattery
Member of the Professional Staff
Meteoritics Department
Systems Group Research Staff

Approved by _____
J. F. Friichtenicht, Manager
Meteoritics Department
Systems Group Research Staff

TRW SYSTEMS GROUP

One Space Park, Redondo Beach, California 90278

TABLE OF CONTENTS

1. Introduction

TRW Systems Group has for the past twelve years been engaged in essentially continuous research programs under NASA sponsorship dealing with laboratory simulation of meteors and of meteoroid impacts on solid surfaces. During this period a large variety of experiments have been performed in which the TRW-developed electrostatic microparticle accelerator and the TRW/NASA microparticle linear accelerator have enabled us to reproduce in the laboratory phenomena not subject (except, perhaps, at extreme expense) to direct scrutiny in situ. Contrary to concerns, occasionally expressed at one time, that such laboratory experiments were irrelevant to the problems of particulate matter in space or in the upper atmosphere, the experiments have now yielded important results in several areas of major scientific and engineering interest: Impact experiments have led to a design for a detector capable of in situ semiquantitative analysis of the composition of cosmic dust, produced significant data relative to the hazards of meteoroid impact on spacecraft structures and components, and generated information which promises to greatly assist the interpretation of microcraters observed in samples of lunar rock. Simulated meteor experiments have improved our understanding of the interactions between high velocity particles and the upper atmosphere and are now approaching a point where their results will improve the accuracy and confidence level of analyses of natural meteor data.

So little is known of the basic physical properties of extraterrestrial particulate matter that measurement of such basic properties as particle masses takes on considerable significance. Various types of impact detectors have been flown or proposed to make the measurement in space. One recent proposal involves the impact ionization effect: It is known that hypervelocity impacts on a suitable solid surface produce free charge proportional to mv^3, where m is the mass and v the velocity of the impacting particle, and it is relatively simple to configure an experiment so that the charge is separated and collected before recombination can occur; also, it is claimed that

the risetime of collected charge depends on v alone and that m can thus be deduced by measuring both the amplitude and the risetime of the collected charge signal. Another--and much older--method of determining the masses of the larger extraterrestrial particles is to study their interaction with the earth's atmosphere in the form of meteors. Since ablation processes are rather well understood, it should only be necessary to know what fraction of the energy of atoms ablated from a meteoroid is converted, by interaction with atoms of the atmosphere, to observable phenomena (usually visible radiation, sometimes an ionized wake) in order to compute m from measurements on those phenomena.

The research discussed in this report directly relates to both types of mass measurement.

2. Impact Ionization Risetime Effect Experiment

Consider first the case of mass determination from an impact ionization analysis. Whereas the proportionality between charge produced at impact and mv^3 is fairly well understood in terms of basic physical theory, the risetime effect has heretofore been an empirical fact without a theoretical basis. As in all such cases, one can (and should) wonder whether the effect is possibly an artifact produced by the configuration of a particular experiment and not by an independent phenomenon. An experiment was therefore undertaken to examine this possibility. The description and results of the experiment were presented in Technical Report No. 16623-6006-RU-00, a copy of which is attached hereto as Appendix A. Those results appear to be quite important because they strongly indicate that the risetime effect is indeed an experimental artifact. The implications are clear: unless some means can be found by which a risetime-effect detector can be calibrated with particles of known properties similar to those expected to be encountered in space, the validity of velocity data acquired by the detector will be highly questionable.

3. Simulated Meteor Experiments

Next consider the way in which meteoroid masses are computed from analyses of photographic meteor data. (The masses so computed are called photometric masses to emphasize the fact that, given the present state of knowledge in the field, they correspond only imperfectly to masses obtained by other means, e.g. radio observations, and presumably to the actual masses of the bodies.) The process essentially consists in numerically integrating the meteor luminosity equation with values of instantaneous velocity and intensity obtained from photographs of the meteor. Since the meteor luminous efficiency--the fraction of the kinetic energy of the ablated meteor atoms that is converted to radiation--is a factor in the luminosity equation, its value must be known before the integration can be performed; and, since meteors vary widely in initial velocity and may decelerate significantly, the luminous efficiency must be known as a function of velocity over the 10-70 km sec^{-1} range of natural meteors.

It is obviously impossible (there being too many unknowns) to evaluate the luminous efficiency from a single meteor observation. Attempts have been made to compute this quantity from statistical treatments of a number of observations. Various investigations have reported different results, and although a relationship evaluating the luminous efficiency as directly proportional to velocity has enjoyed wide currency, its validity has been energetically challenged by several workers. Given a situation such as this one in which the phenomenon in its natural form is only marginally accessible for quantitative study but is quantitatively well understood, the possibility and the advantages of investigating it indirectly under controlled laboratory conditions are both great. For reasons of simplicity such experiments have dealt almost exclusively with single elements known (from meteor spectra) to be constituents of natural meteoroids. This is not necessarily a handicap, since if we understand the phenomenon as claimed we can synthesize the effective luminous efficiency of a complex particle

from those of its constituent elements and can study the effect of differences in composition on the aggregate luminous efficiency. It must be admitted that the accuracy of the synthesis depends upon our knowledge of the composition of natural meteors and that the state of that knowledge is barely adequate to the task; but this is not a fundamental problem, and there is every expectation that it will ameliorate given time and further research.

One useful type of experiment is the measurement of emission cross sections for collisions between single atoms of meteoroid constituents and molecules of atmospheric gases. Crossed atomic beam techniques are required for such measurements and have been employed by several researchers. Experiments of this kind are invaluable because they reduce the gross phenomenon to the level of initial causality. Unfortunately, methods currently in existence for producing atomic beams can only be employed with a few constituent elements of meteoroids, usually the easily-ionized ones such as sodium, potassium, magnesium and calcium. (Moreover, the computation of luminous efficiency from cross section data is an involved procedure involving a number of simplifying assumptions which conceivably may affect the accuracy of the final results). An alternative is to accelerate microscopic particles to meteoric velocities in the laboratory and to allow them to interact with a gaseous atmosphere. This permits the phenomenon to be examined directly at the macroscopic level. By using particles with diameters below a few microns, free molecule flow conditions simulating those encountered by a meteoroid entering the earth's upper atmosphere are readily achieved at pressures of a few tenths of a Torr. Not only are such pressures easily controlled and measured, but also they result in a reasonably small spatial extent for the phenomenon; a typical simulated meteor emits all of its radiation over a trail length of 50 cm or thereabouts, which is easily contained within laboratory apparatus of practical size. At one time there existed some concern that absolute pressure, rather than relative pressure expressed in terms of flow conditions,

was an important factor in the simulation and that in the laboratory quenching of certain excited states might occur in a way not duplicated in actual atmosphere entry. Although the question has not been definitively answered, it has been found that laboratory results for the luminous efficiency of iron compare quite well with those obtained by rocket-injecting iron spheres into the atmosphere to produce artificial meteors with velocities around 10 km sec^{-1}. Hence the evidence to date is that the simulation is a good one. It should be noted that an important advantage of this method is that it can best be used with just those metallic constituents of natural meteoroids which are not now amenable to atomic beam generation in the required velocity range--iron, silicon, nickel, aluminum, etc.

Laboratory meteor simulation as a practical experimental technique was pioneered by TRW Systems Group under NASA sponsorship. Prior work in the field has included: drag and heat transfer measurements on simulated micrometeoroids; measurement of the ionizing efficiencies of a variety of meteoroid materials over very wide velocity ranges; determination of the emission spectrum of simulated iron meteors; measurement of the luminous efficiency of iron ablating in air for velocities from 10 to 48 km sec^{-1}; and measurement of the emission spectrum and luminous efficiency of copper in order to begin interelemental comparisons. Under the current program the work has continued with the measurement of the luminous efficiencies of silicon and aluminum in air, nitrogren, and oxygen atmospheres and at velocities camparable to those of the earlier work with iron. The experiment was fully described in Technical Report No. 16623-6007-RU-00, a copy of which is appended and designated Appendix B; a version of this report is to be submitted for publication in an appropriate journal.

We have also in this report attempted to utilize the data now in existence for elemental luminous efficiencies (data generated in part during this research program, in part during earlier programs, and in part by other investigators) to synthesize the luminous

efficiency of a composite meteoroid. Although tentative, the result is important because it contradicts the hypothesis that luminous efficiency increases in direct proportion to velocity. The composite value behaves instead much like the luminous efficiency of any one element: after rising to a peak with increasing velocity, it declines with further velocity increases. The peak appears to occur at about 25 km sec^{-1}, beyond which the luminous efficiency is almost proportional to 1/v. This implies that over most of the natural meteor velocity spectrum the "law" of proportionality to v may not be valid, which implies in turn that many photometric masses already determined may be subject to modification. However, we tend to believe that in view of the fairly revolutionary nature of this finding, total acceptance should be held in abeyance pending further corroboration.

4. Suggestions for Further Work

Our impact ionization experiment did not find that velocity determination from the detailed behavior of ionization signals is impossible; rather, by showing that the risetime effect is produced by an interaction between the impact phenomenon and the experiment geometry, we have argued that laboratory studies using solid, dense particles are not adequate to calibrate for velocity measurement in situ. There remains the possibility that a systematic study of spray particle production under various conditions of particle material and impact surface composition may reveal regular variations that could be used for such a calibration.

In the area of meteor luminosity, an obvious and important experiment would be the measurement of the luminous efficiency of magnesium by the simulated meteor method. Magnesium is suggested because there exist luminous efficiency values for this element derived from atomic beam cross section studies and because there is a chance (better, we estimate, than 50 percent) that magnesium may be made to operate in our simulated meteor acceleration system. Hence it would be possible to directly compare luminous efficiency

values obtained by two very different methods. Agreement, if found, would greatly increase the confidence level of both kinds of experiment.

Since most elemental constituents of meteoritic stone are likely to be present as compounds rather than in pure form, there may be some interest in studying the relationship between the luminous efficiency of a compound material as compared to the efficiencies of its constituents. There are several possible candidates for such a study; an example is ferrous metatitanate ($FeTiO_3$), which seems attractive due to the fact that the compound itself, iron, and titanium have all been successfully accelerated to meteroic velocities in our apparatus.

A major source of uncertainty in the synthesis of meteor luminous efficiency from elemental values is that the synthesis depends upon our still very uncertain knowledge of the relative mass abundances of elements in meteoritic stone. A simple "paper experiment" would be to treat the elemental luminous efficiencies as givens and the relative abundances as variables in order to determine how the latter can affect the synthesized result. Such an experiment might employ digital computation techniques and need not be very extensive in terms of manpower or cost.

Finally we note that the current research program did not include further examination of ionizing efficiencies or of heat transfer coefficients. Techniques already developed for those measurements could easily be applied to silicon, aluminum, magnesium, and other materials of interest to the meteor problem. The results could lead to an improved understanding of radiometeor processes and could check the validity of heat transfer assumptions employed in the reduction of data from both simulated and natural meteors.

Appendix A

16623-6006-RU-00

RISETIME EFFECTS IN IMPACT IONIZATION METEOROID DETECTORS

J. C. Slattery

December, 1972

Technical Report

Prepared Under

Contract NASw-2246

For

NATIONAL AERONAUTICS AND SPACE ADMINISTRATION

Headquarters

Washington, D.C. 20546

TRW SYSTEMS GROUP

One Space Park, Redondo Beach, California

(-a

RISETIME EFFECTS IN IMPACT IONIZATION METEOROID DETECTORS

J.C. Slattery

Abstract

The impact ionization effect is used in the design of micrometeoroid sensors for space research, and some designs distinguish "slow" from "fast" impacting particles by measuring the risetime of the ionization signal. The ionization signal risetime from "slow" particles experimentally is different than that from "fast" particles. This report describes an experiment to discover the origin of that difference. It is concluded that the effect is due to the experimental geometry and certain details of particle composition. It is not inherent in the impact ionization phenomenon.

RISETIME EFFECTS IN IMPACT IONIZATION METEOROID DETECTORS

1. INTRODUCTION

The impact ionization effect--the production of free charge at the impact site of a hypervelocity particle on a suitable target--was first described in a research note from this laboratory several years ago.[1] It appears that the impact creates temperatures high enough not only to vaporize the particle and some of the target material but also to thermally ionize a fraction of the vaporized atoms. The result, it is believed, is a microplasma, from which charge may be extracted through the application of electric fields. Although the process has not yet been directly observed, and consequently the details of the mechanism remain somewhat uncertain, a large and growing body of indirect evidence[2,3] points to the fact that this description is essentially correct.

The signals resulting from the extraction of charge (ions, electrons, or both) from the microplasma can be utilized in a variety of ways to deduce certain properties of the impacting particle. Two important examples are a micrometeoroid detector[4] and an instrument which measures the composition of impacting materials by accelerating the impact ions and then measuring their flight times over a known distance in order to determine the identity of the species from their atomic masses.[5] Both kinds of instrument share the same basic configuration: a grid is located close to the impact surface and parallel to it, and an electric field is imposed between grid and target to separate and collect the impact charge. When the charge collected at the target is then observed, two components are often noticed, separated in time by a few microseconds. The earlier component, which occurs at the instant of impact, is always present, but the later one is only seen for impact velocities below about 10 km/sec. It thus seems that one could detect the presence or absence of the second component (in practice, the risetime of the target signal would be measured and the presence of the second component would be given by the appearance of a slow risetime) and infer therefrom the impacting particle velocity. Several micrometeoroid impact detectors which make use of this effect have in fact been designed and constructed.

In this report we discuss the results of a simple experiment undertaken to examine the causes of the two-charge-component effect. The results were unambiguous and rather surprising: the effect is due to the experimental geometry and to certain details of particle composition. This implies that using the effect for measurement of particle velocities has some major limitations and uncertainties of which investigators should be aware.

2. EXPERIMENTAL ARRANGEMENT

A schematic of the experimental arrangement is shown in Figure 1. A test particle, incident from the left, passes through a particle detector, then a shield grid, then an accelerating grid, and finally impacts the target on the right in the schematic. Because of the voltage on the accelerating grid, ions leave the target. The resultant signal is observed with amplifiers at the target. As shown in the schematic, the target is divided into two parts, electrically isolated from each other. The inner target is circular, about 3 mm in diameter, and its face is flush with the outer target. Both inner and outer targets are tantalum. The incoming particle impacts the inner target and it is here that the impact ionization charge is created.

Two different accelerating grid structures were used in the experiments, as indicated in Figure 1. The "open" grid is a 1.6 cm diameter hole, with 0.005 cm tungsten grid wires, spaced 0.25 cm apart in two dimensions. This is a very high transmission grid. The "closed" grid is not really a grid, but rather a solid plate (tantalum) with a 3 mm diameter hole in it. When the "closed" grid was used the hole was centered on the inner target (and also the particle trajectory). Grid to target spacing was 0.63 cm with either grid and an accelerating potential of -400 volts was applied to the grid.

Test particles were micron-sized iron spheres accelerated by the TRW Systems 1.5 MV particle accelerator. The particle detectors measure the charge on the particle from the voltage height of the detector signal and the known input capacitance of the detector-amplifier and the known gain of the amplifier. In this case particle velocities were calculated from the measured transit time between the particle detector and the

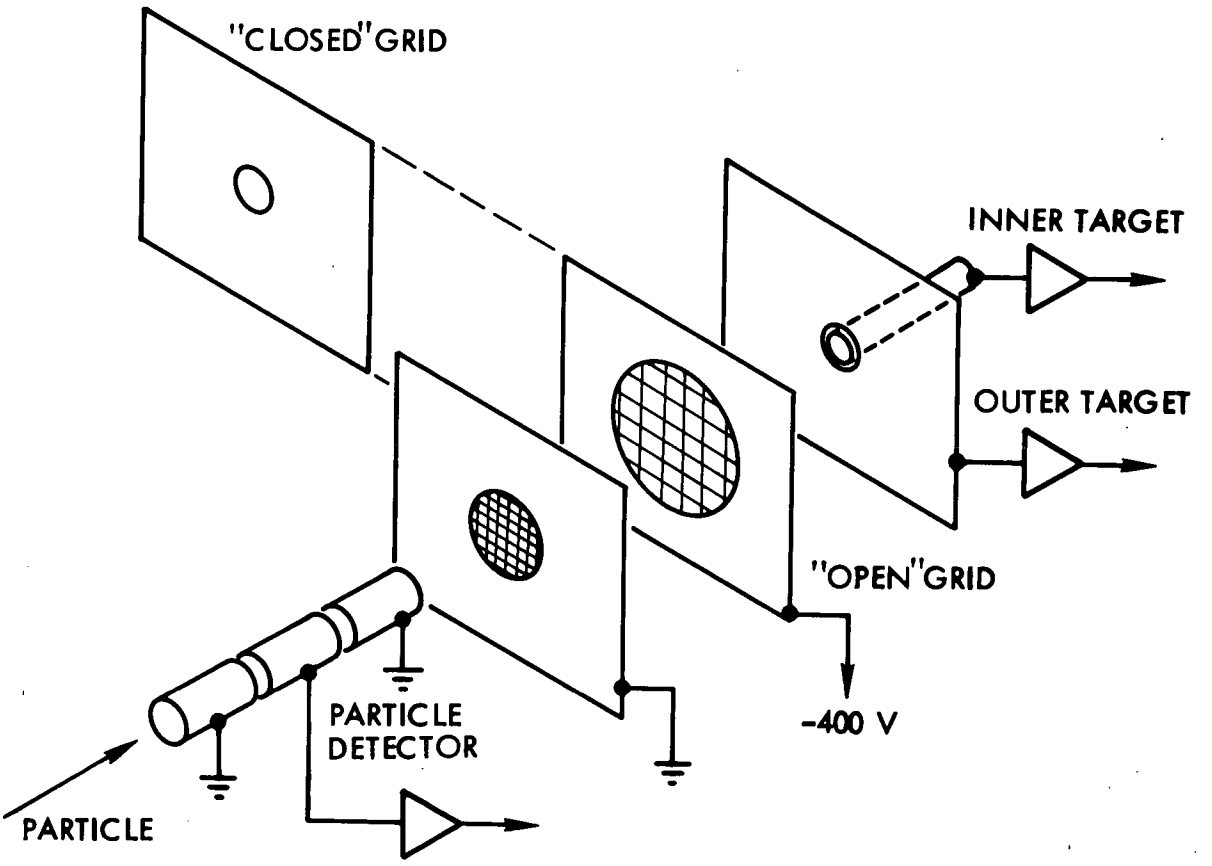

Fig. 1. Schematic representation of arrangement of impact ionization risetime effect experiment. Outputs of two target amplifiers are fed to a dual-beam oscilloscope. Photographic oscillograms are analyzed later.

impact target. Given the particle charge Q, velocity v, and the accelerating potential U, the mass m is calculated from

$$QU = mv^2/2 \qquad (1)$$

A dual trace oscilloscope was used to record the data, with both traces running at the same sweep speed. The signals from the particle detector and inner target amplifier were added and displayed on the upper trace, while the outer target amplifier signal was displayed on the lower trace.

Figure 2 shows tracings of oscilloscope pictures of typical events. In Figure 2a and 2b the inner and outer targets are electrically connected and the two target amplifier signals are virtually identical because the amplifiers have the same gain and frequency response. The "closed" grid was used for both 2a and 2b. The impacting particle in Figure 2a had a velocity of 5.6 km/sec, a mass of 9.7×10^{-16} kg, and a radius of 3.1×10^{-7} meters. The target amplifier signals show the two component behavior typical of slower particles. The target signal goes slightly positive as the positively charged particle approaches and then negative at impact as ions leave. After a delay of about 2 or 3 microseconds a second, larger, charge burst is seen. It is either more positive charge leaving or negative charge arriving. The sweep speed is 5 μsec/div, vertical sensitivity 0.2 volts/div for the particle detector amplifier signal, and 0.1 volts/div for the two target amplifier signals.

In Figure 2b the impacting particle is faster. It has a velocity of 14.3 km/sec, a mass of 7.7×10^{-17} kg, and a radius of 1.3×10^{-7} meters. These numbers are obviously approximate because the particle detector signal is too small to make very accurate measurements. Still, the particle in Figure 2b is clearly faster and smaller than the one in Figure 2a. The target amplifier signals in Figure 2b are more or less typical of faster particles, showing a (relatively) large immediate charge burst and a very small delayed charge burst. Sweep speed and vertical sensitivities are the same as in Figure 2a.

In Figures 2c and 2d the inner and outer targets are no longer connected. The inner target amplifier signal is on the top trace and the

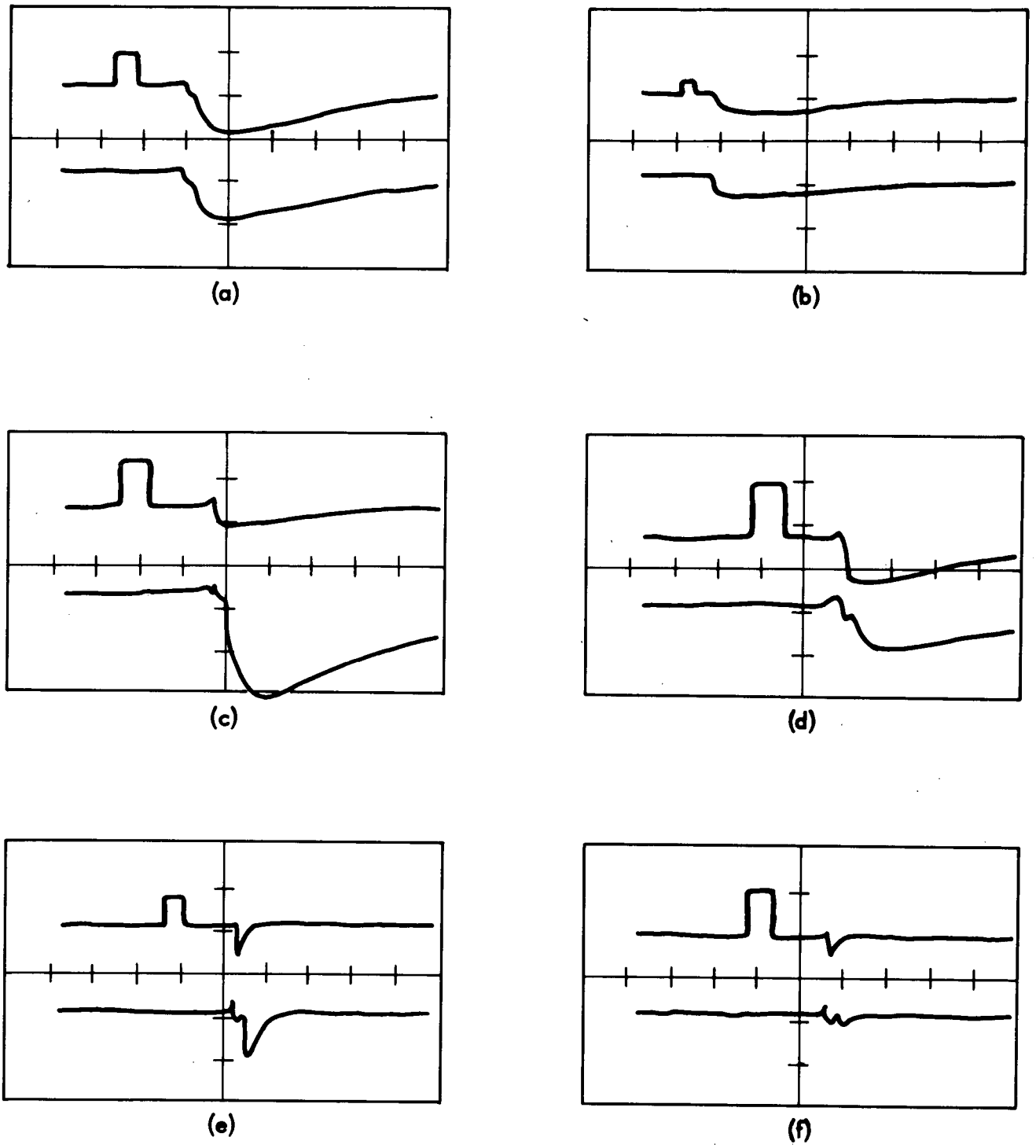

Fig. 2. Typical oscillograms produced by different particle velocities and experimental configurations. For all cases the following apply: vertical sensitivity, 0.2V/division for particle detector, 0.1V/division for both target signals; sweep speed, 5 μsec/division.

outer target signal on the lower trace. The "closed" grid was used in Figure 2c. The impacting particle had a velocity of 4.1 km/sec, a mass of 4.7×10^{-15} kg, and a radius of 5.2×10^{-7} meters. Sweep speed is 5 μsec/div and vertical sensitivities the same as in Figures 2a and 2b. The impact was on the inner target and note that this signal shows only the immediate charge burst, with no delayed component. There is a delayed charge burst but it is on the outer target only. This delayed charge burst continues to rise for almost 5 μsec, in contrast to the immediate charge burst which has a short risetime. The sharp spike on the outer target signal, coincident with the inner target signal, is due to the sudden appearance of free ions in the grid-target space, where they induce a signal on the outer target capacitance.

In Figure 2d the "open" grid has been substituted for the "closed" grid and there is less grid material directly in front of the target. Sweep speed and vertical sensitivities are the same as in Figure 2c. The impacting particle had a velocity of 4.7 km/sec, a mass of 2.4×10^{-15} kg, and a radius of 4.2×10^{-7} meters. The signals again show the immediate charge burst on the inner target only and a delayed charge burst on the outer target only. However, the relative magnitudes have been changed by the use of the "open" grid. With the "closed" grid (Figures 2a and 2c) the delayed charge component is consistently a factor of 2 or 3 larger than the immediate component. In Figure 2d they are more nearly equal.

This same general behavior is shown in a slightly different way in Figures 2e and 2f. The RC time constant at the inner and outer targets has been made about 0.13 μsec (12 pf and 11 k ohms) and so the signals show current at the targets rather than voltage. Figure 2e is the "closed" grid case. The impacting particle had a velocity of 5.4 km/sec, a mass of 1.3×10^{-15} kg, and a radius of 3.5×10^{-7} meters. Immediately after the impact there is a short burst of current on the inner target only and after a delay of about 2 μsec there is a (larger) burst of current on the outer target. This delayed current on the outer target is seen to last for a longer time than the short burst on the inner target.

Figure 2f illustrates the "open" grid case. The particle had a velocity of 4.7 km/sec, a mass of 2.04×10^{-15} kg, and a radius of 4.0×10^{-7} meters. The behavior of the current at the two targets is

similar to Figure 2e except that now the delayed current is (relatively) much smaller than was the case with the "closed" grid, Figure 2e.

3. CONCLUSIONS

The following conclusions may be reached from the data above. For particles with velocities under about 10 km/sec, the impact ionization charge signal shows two components. The first component follows immediately the impact and its origin is close to the impact site. A second component is observed which is delayed by about 2 μsecs from the first and it is charge collected (or emitted) on the target some distance from the impact site. The relative amount of this delayed charge is dependent on the amount of material in front of the target, with an "open" structure causing less delayed charge.

The explanation for these facts is illustrated schematically in Figure 3a, the "closed" grid case, and Figure 3b, the "open" grid case. Iron particles impacting a solid surface at low velocities (less than about 10 km/sec) tend to fragment and to throw back small "spray" particles. There is particle vaporization, but the charge produced per unit mass of impacting particle is a steep function of velocity (approximately proportional to the fourth power of the velocity). Thus, the higher velocity particles are more completely vaporized and produce either much smaller or many fewer spray particles. It is these spray particles which create the delayed charge component.

A spray particle thrown back from the original impact site at a velocity of 5 km/sec will cross the 0.63 cm grid-target spacing in about 1.3 μsec. If it impacts a solid material, it will create a second impact ionization plasma. The electric field is still present and charge of the appropriate sign is drawn to the target. There are many of these small spray particles and those which come off the impact site at larger angles have a longer distance to travel before striking the grid. The consequent range of travel times accounts for the long rise time of the delayed charge component. Because the spray particles must hit a surface where an electric field is present in order to produce the delayed charge, "open" grid structures give rise to less delayed charge.

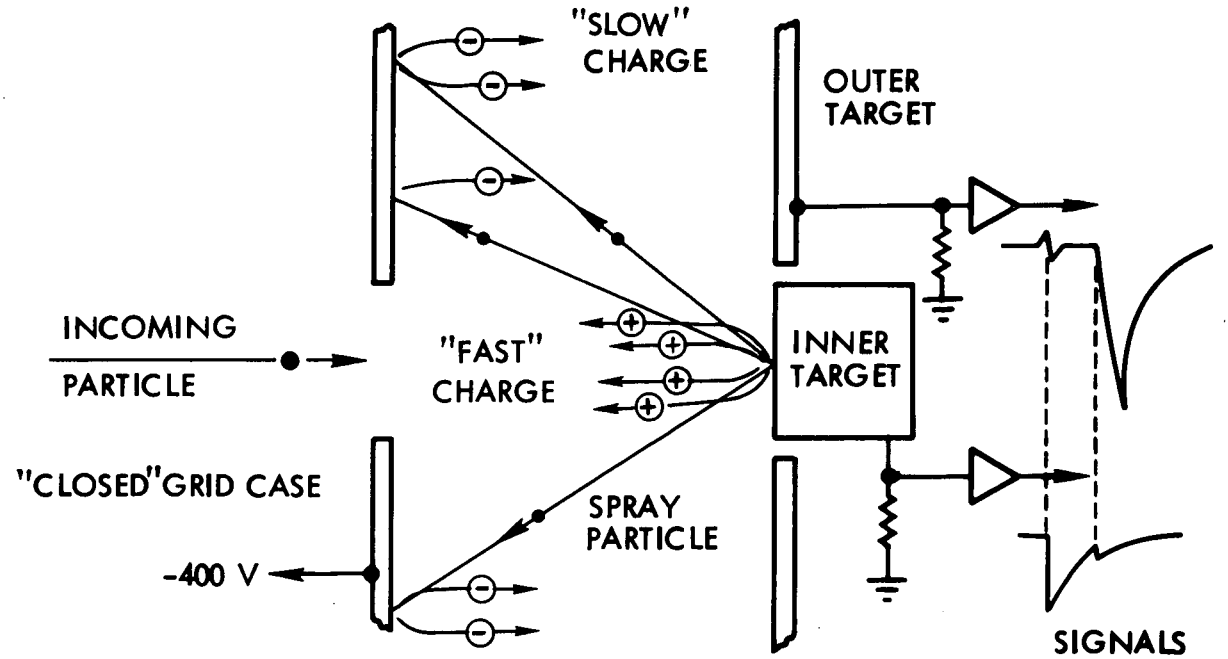

(a)

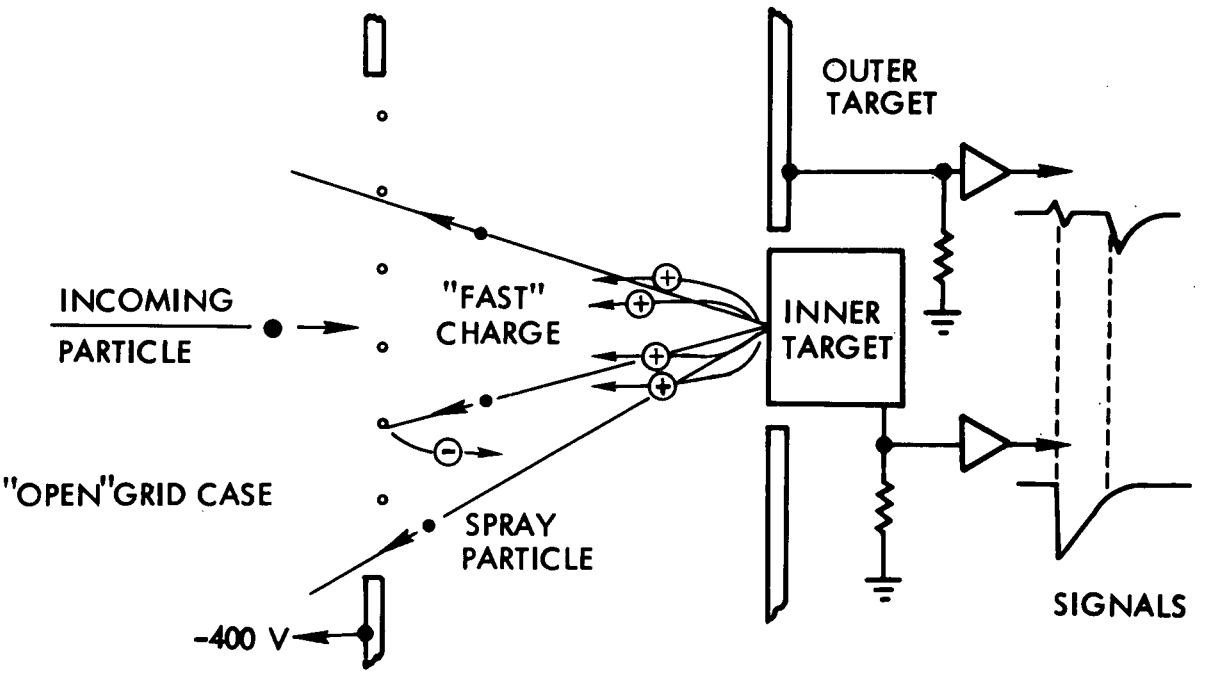

(b)

Fig. 3. Schematic representation of the interaction between experiment geometry and spray particle production. Note that the distribution of "fast" and "slow" charge is identical in (a) and (b), but the "open" grid structure in (b) reduces the likelihood of spray particle impacts.

Certain considerations in the design of impact ionization micrometeroid detectors now become obvious. Those detectors which depend on measurement of the signal risetime to indicate the impacting particle velocity should be used with care. The fact that the phenomenon is strongly geometry-dependent would not be serious if the design could be tested in the laboratory with particles of the same material as those to be detected in space. This laboratory testing should concern itself particularly with the effect of different angles of impact. The velocity and emission direction of spray particles varies in an unknown way with angle of impact. Even at a constant impact angle, the detector signal is likely to depend on the exact location of the impact on the target.

The dividing line of 10 km/sec between slow particles exhibiting a delayed charge burst and fast particles which do not is based mainly on experiments with iron spheres of a particular size (less than 1 micron radius). The behavior of particles of radius 10 or 100 microns may be quite different. The effect of various particle materials and structures is difficult to assess and impossible to measure in the laboratory because the composition and structure of particles encountered in space is not known. Stone particles of a porous structure may throw back few spray particles at any velocity. Low density, compact particles may emit spray particles at velocities well over 10 km/sec.

Because of the many uncertainties involved, we conclude that particle velocity measurements based on the character of the impact ionization signal should be treated with great care.

REFERENCES

1. J.F. Friichtenicht and J.C. Slattery, NASA Technical Note, TN-D2091 (1963).

2. D.O. Hansen, Appl. Phys. Letters, 13, 89 (1968).

3. N.L. Roy and D.G. Becker, "Design Fabrication, and Test of the Breadboard Unit of the Cosmic Dust Analyzer Experiment: Final Report," TRW Systems Doc. No. 10735-6001-RO-00 (1970).

4. S. Auer and K. Sitte, Earth and Plan. Sci. Letters, 4, 178 (1968).

5. J.F. Friichtenicht, N.L. Roy, and L.W. Moede, "Cosmic Dust Analyzer: Final Report," TRW Systems Doc. No. 10735-6002-RO-00, (1971).

Appendix B

16623-6007-RU-00

LUMINOUS EFFICIENCY MEASUREMENTS FOR SILICON AND ALUMINUM SIMULATED MICROMETEORS

D.G. Becker and J.C. Slattery

December, 1972

Technical Report
Prepared Under
Contract NASw-2246

for
NATIONAL AERONAUTICS AND SPACE ADMINISTRATION
Headquarters
Washington, D.C. 20546

TRW SYSTEMS GROUP
One Space Park, Redondo Beach, California

1-a

LUMINOUS EFFICIENCY MEASUREMENTS FOR SILICON AND ALUMINUM SIMULATED MICROMETEORS

D. G. Becker and J. C. Slattery

ABSTRACT

Laboratory measurements on simulated silicon and aluminum micrometeors in an air atmosphere have produced values for the elemental photographic luminous efficiencies τ_{pg}(Si) over a velocity range 13-48 km sec^{-1} and τ_{pg}(Al) over a range 12-42 km sec^{-1}. We found that both behave as functions of velocity much like τ_{pg}(Fe) and τ_{pg}(Cu) described in an earlier paper: τ_{pg} first increases with increasing velocity, then reaches a peak and declines. Peak values are τ_{pg}(Si) = 3.5 x 10^{-13} sec erg^{-1}, 0 mag at 24 km sec^{-1} and τ_{pg}(Al) = 4.8 x 10^{-13} sec erg^{-1}, 0 mag at 22 km sec^{-1}. Supplementary measurements on Si and Al in atmospheres of O_2 and N_2 support the air results. Comparison with τ_{pg} for Fe and Cu and for Mg and Ca obtained by other investigators using atomic beam techniques reveals a trend toward lower peak velocity with increasing atomic mass. We combine all of these data to get a tentative τ_{pg} for natural meteors; the result varies with velocity roughly as v^{-1}, which suggests that the natural meteor luminous efficiency "law" $\tau_{pg} = \tau_{op}v$ may not be as certain as once believed.

LUMINOUS EFFICIENCY MEASUREMENTS FOR SILICON AND ALUMINUM SIMULATED MICROMETEORS

D. G. Becker and J. C. Slattery

I. INTRODUCTION

The reduction of data from photographic meteors involves the deduction of the elementary physical properties of the meteoroid at atmospheric entry--notably the initial mass m_o--from measurements of meteor luminous intensity and velocity. These quantities are related by the luminosity equation

$$I_{pg} = -\frac{1}{2}\tau_{pg} v^2 \, dm/dt \quad , \qquad (1)$$

where dm/dt is the rate of mass ablation, v is the instantaneous velocity, I_{pg} is the total intensity of radiation emitted within the spectral response of the meteor camera (the subscript pg refers specifically to a Super-Schmidt camera employing a blue-sensitive emulsion such as Kodak 103a-O), and τ_{pg}, the photographic luminous efficiency, is the fraction of the total kinetic energy of atoms ablated from the meteoroid which is converted into radiation within that spectral response. Before m_o can be determined by integration of (1), the value of τ_{pg} must be known.

Attempts to infer τ_{pg} directly from meteor observations[1] have been somewhat less than satisfactory, in the sense that practitioners of this method have apparently been unable to reach a consensus regarding either the proper treatment of the raw data or the interpretation of the results of the analyses. Hence there has been a growing interest in laboratory experiments which measure τ_{pg} for elemental meteor constituents. At present such experiments are of two kinds: direct measurements on simulated micrometeors, originated by Friichtenicht, Slattery, and Tagliaferri[2] and refined by Becker and Friichtenicht,[3] and emission cross-section measurements employing atomic beam techniques, as reported by Boitnott and Savage[4,5] and by Neff.[6] The first kind of experiment is most useful with metallic elements that are not excessively reactive (iron, aluminum,

silicon, possibly magnesium), whereas the second kind--given existing limitations of atomic beam technology--is applicable to the alkali metals and alkali earths (sodium, potassium, magnesium, calcium). Together, therefore, these experimental techniques permit the measurement of τ_{pg} for all meteor constituents found to be significant emitters of radiation in the photographic spectrum.[7] Once this task has been accomplished, it should be possible to synthesize τ_{pg} for a meteor from elemental τ_{pg} values weighted according to relative abundance.

We discuss in this paper laboratory measurements of τ_{pg}(Si) and τ_{pg}(Al) obtained by the simulated micrometeor technique. Our data give the luminous efficiencies in both physical units (dimensionless) and magnitude units (sec erg^{-1}, 0 mag), as functions of velocity from 13 to 48 km sec^{-1} for silicon and from 12 to 42 km sec^{-1} for aluminum. These results are compared directly to τ_{pg}(Fe) determined by Becker and Friichtenicht and to τ_{pg}(Mg) and τ_{pg}(Ca) computed by Boitnott and Savage. (Note that sodium and potassium are not significant radiators within the blue-sensitive photographic spectrum, although both become important for detectors whose spectral response extends to longer wavelengths). We also present emission spectra for silicon and aluminum simulated micrometeors; these were required for reduction of the τ_{pg} data. Finally, we offer an initial attempt at a synthesis of the photographic luminous efficiency of a natural meteor from the elemental τ_{pg} values.

II. EXPERIMENTAL METHOD

With a few relatively minor exceptions, the experimental approach was identical to that employed by Becker and Friichtenicht, which is described in considerable detail in Reference 3. For this reason we present herein only a brief summary of the method.

a) Data Acquisition

Microparticles of the appropriate material (silicon or aluminum; typical particle diameters were 0.05-1.0 μ) were electrically charged and accelerated in vacuo in a 2-MV Van de Graaff generator modified for this application.[8] The velocity v_o and charge q of each particle were measured by detectors;[9] given the accelerating voltage V_a, the total kinetic energy

E_o and mass m_o were computed ($E_o = qV_a$ and $m_o = 2E_o/v_o^2$). After triggering electronics which insured that data were recorded only if v_o was within the range of interest, [10] the particles passed through a set of differential pumping apertures and entered a target gas region 60 cm long, in which they ablated and produced the luminous trials that we refer to as simulated meteors. The trails were observed by a main PMT and an auxiliary PMT (both Centronic P4282B, a change from the RCA 8575 and Centronic P4242B used by Becker and Friichtenicht) placed on opposite sides of the target chamber. Both tubes were located on a common centerline perpendicular to the trajectory of the meteors and intersecting it 20.9 cm from the target chamber entrance aperture. The target gas (air, nitrogen, or oxygen) was maintained at a pressure such that the peak intensity of the luminous trail occurred at about 20 cm from the chanber entrance (i.e., when the ablating particle was almost directly opposite the PMT's), since under this condition all of the radiation from the meteor would be emitted within the field of view of the photodetectors; the requisite pressure, a function of v_o, was empirically determined for each velocity range of interest and was typically $\sim$0.2 Torr (which resulted in free molecule flow for all particle sizes of concern to us). The combined spectral response of a PMT and its lucite window extended from 3400 to 5800 Å.

The output of the main PMT was integrated electronically, and its magnitude was then proportional to total radiant energy. The anode time constant of the auxiliary PMT, however, was made short enough that this tube responded directly to radiant intensity. This step--a departure from Becker and Friichtenicht's method, where the auxiliary PMT output was also integrated--was taken in order to obtain better control over the length of the trail. Figure 1 is a typical record of a single event; it is an oscillogram made with a dual-beam oscilloscope (Tektronix 555), with the outputs of two particle detectors and the auxiliary PMT added together on the top trace and the integrated output of the main PMT on the bottom trace. The "notches" apparent in the auxiliary PMT signal were produced by opaque markers located at 14.7 cm and 23.0 cm (measured along the meteor trajectory) from the target chamber entrance. In order for a datum to be acceptable, we required that the peak detected radiant intensity occur between the markers. (The datum in Figure 1 just met

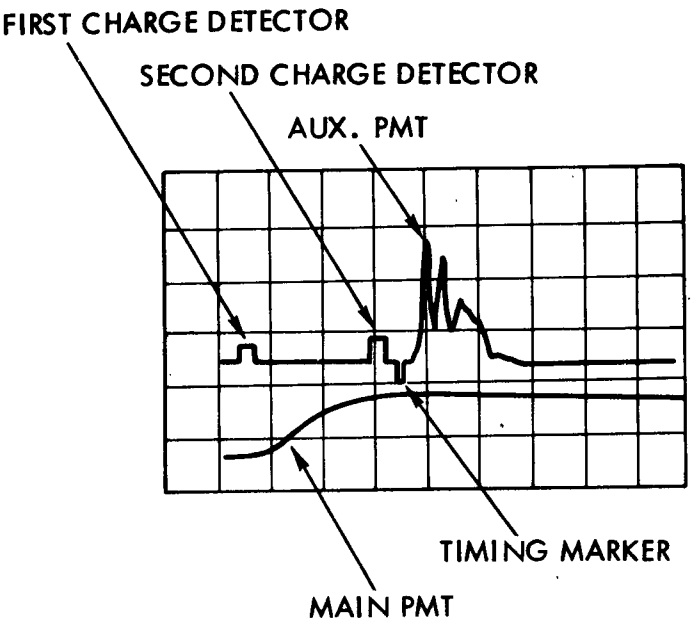

FIG. 1.--A typical oscillogram from the experiment, obtained with the experimental setup described in Ref. 3, a Tektronix 555 oscilloscope, and a trace-recording camera. Two particle charge detector outputs and the auxiliary PMT output are displayed on the upper trace, which begins shortly before particle enters first detector; physical spacing between detectors was 90.9 cm. "Notches" visible on auxiliary PMT trace are caused by opaque markers which help to locate point of peak trail intensity. (In this case that point occurred just as the particle reached the first marker; if sooner, the datum would have been rejected.) The lower trace displays the main PMT output and begins when the timing marker on the upper trace appears. Particle detector signals provide means to determine v_o, m_o, and E_o; amplitude of lower trace gives photo-charge Q. Oscilloscope deflection factors were: 0.1 V/division for both particle detectors, 1.0 V/division for auxiliary PMT, 10 V/division for timing marker, and 1.0 V/division for main PMT; sweep speeds were 20 μsec/division upper trace, 10 μsec/division lower trace.

this requirement.)

The average emission spectra for silicon and aluminum simulated micrometeors were needed in order to reduce the luminous efficiency data. Spectra were obtained exactly as described for iron by Tagliaferri and Slattery,[11] with one difference: rather than only two PMT's, we employed five, all located at the same distance from the entrance into the target gas region with all photocathodes equidistant from the meteor trajectory. Four of the tubes--an RCA 8575, two Centronic P4282B's, and a Centronic P4242B--were fitted with narrow-band interference filters, while the fifth--an RCA 6199--was operated unfiltered and used to normalize the outputs of the other four for variations in total radiant output from one simulated meteor to the next.

b) Data Reduction

Relative spectral intensities $f(\lambda)$ were computed for silicon and aluminum as described in Reference 11. For both materials some minor systematic differences were noted between "low velocity" (< 20 km sec^{-1}) and "high velocity" (> 20 km sec^{-1}) simulated meteors, and so the data were segrated by velocity regime prior to averaging. Figures 2 and 3 are respectively the emission spectra for silicon and for aluminum. The figures also give the emission spectra modified by folding in the relative response $P(\lambda)$ of a standard blue-sensitive photographic detector. Only integrals of these spectra over wavelength were required in the reduction of luminous efficiency data, and although we computed these separately for each velocity regime we discovered that the differences were not significant within the estimated accuracy of the measurement; hence only a single spectral integral sufficed for reduction of data for each material.

The remainder of the data reduction procedure was generally in accord with that discussed in Reference 3. The photographic luminous efficiency was to be determined from

$$\tau_{pg} = E_{pg}(E_o - 2\zeta m_o)^{-1} \quad , \qquad (2)$$

where E_{pg} is the total radiated energy within the blue-sensitive photographic passband, E_o is the initial energy of the simulated meteoroid

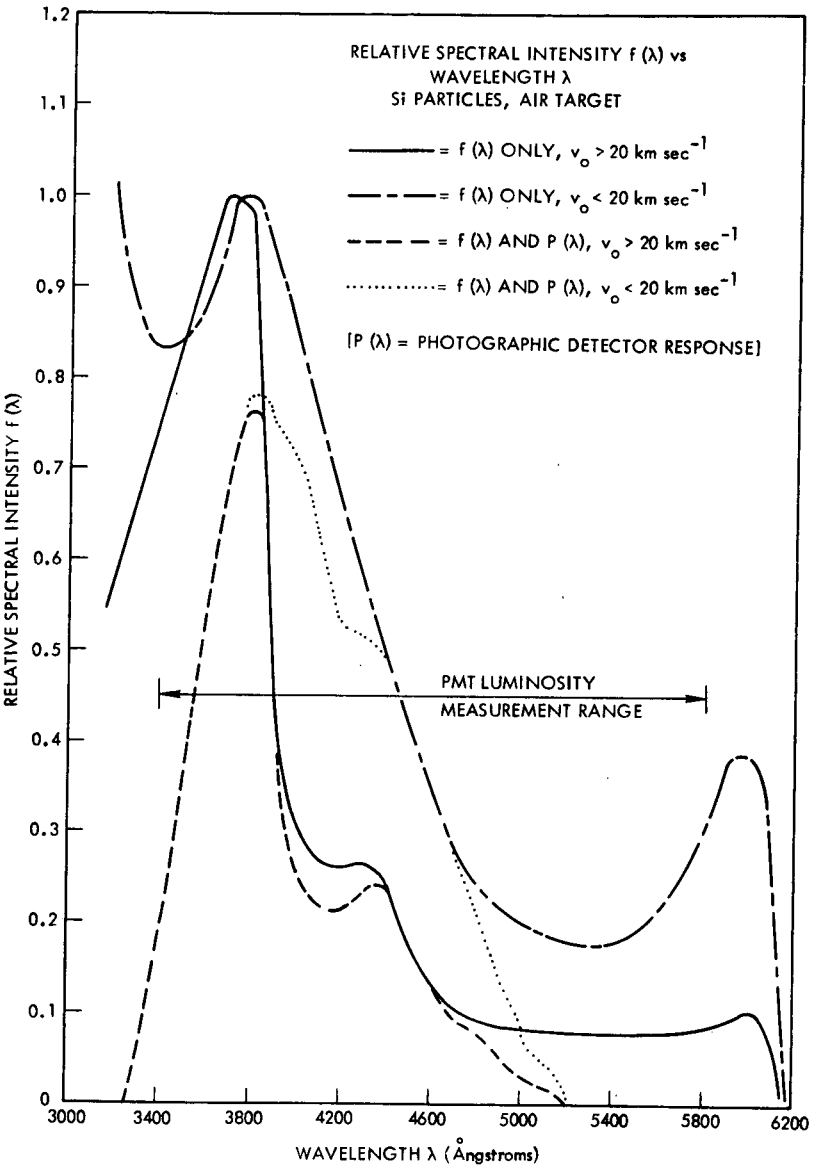

FIG. 2.--Spectrum of light emitted from silicon simulated meteors, showing the PMT response range for the present experiment and the effect of the response characteristic of a standard blue-sensitive meteor camera. Data were obtained as described in Ref. 11.

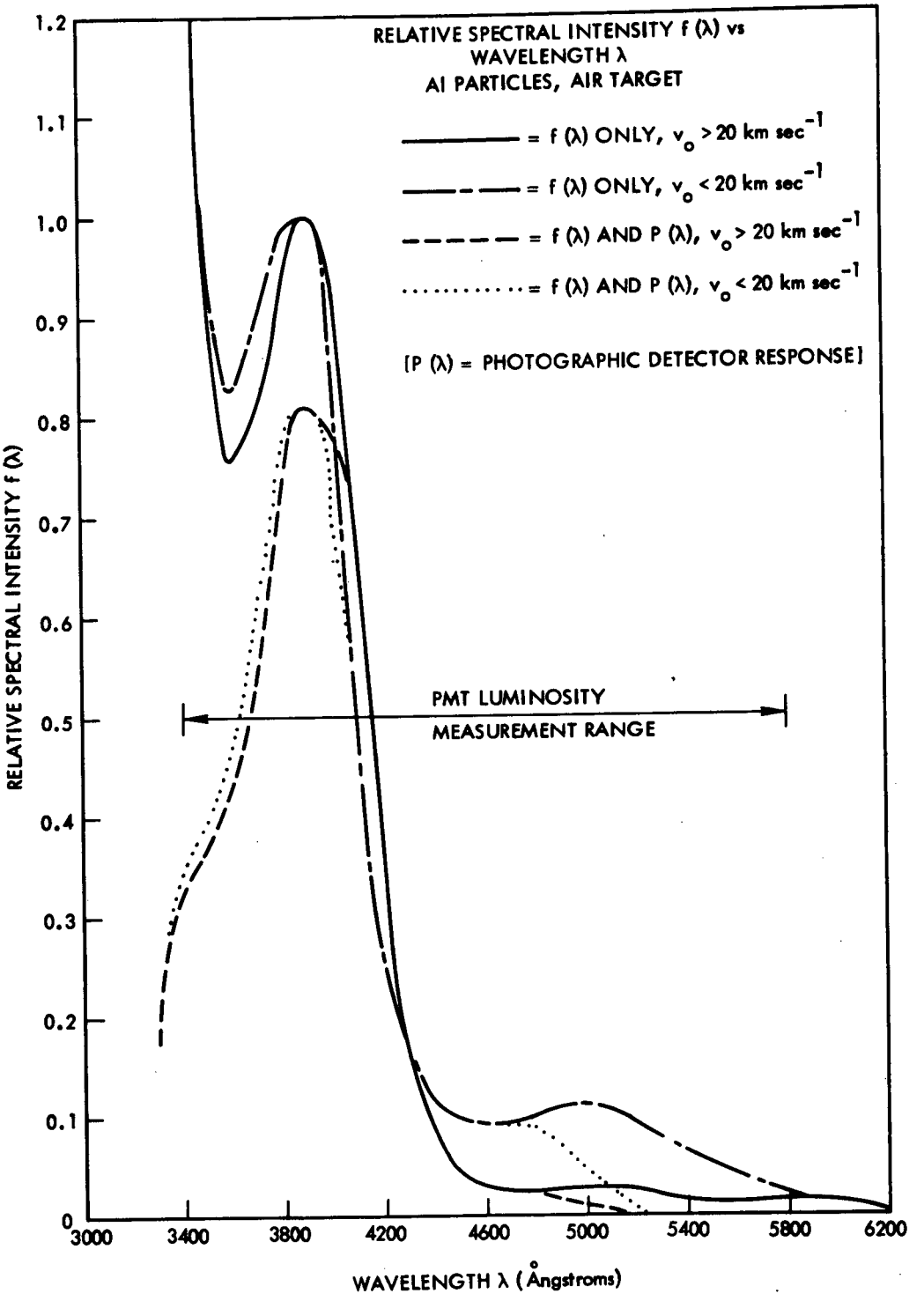

FIG.3.--Spectrum of light emitted from aluminum simulated meteors.

prior to the onset of ablation, m_o is the initial mass, and ζ is the heat of ablation. Since ablation could be assumed to occur by vaporization, ζ was merely the sum of the heats of fusion and vaporization for the material: 1.22×10^7 joules kg^{-1} for silicon, 1.09×10^7 joules kg^{-1} for aluminum. We have already seen that measurements on the particle prior to its entry into the target chamber provided for the computation of E_o and m_o; therefore the problem of data reduction become the computation of E_{pg} from the total integrated photo-charge Q collected by the main PMT.

Let E'_{pg} denote the radiant energy that would have been collected by the main PMT if it had had a relative spectral response $P(\lambda)$ identical to that of the conventional blue-sensitive meteor camera. (That response function is zero for $\lambda < 3300$ Å and $\lambda > 5200$ Å; its value between these limits is tabulated by Allen.[12]) Let $g(\lambda)$ represent the actual relative spectral response of the main PMT and $h(\lambda)$ the transmittance of the lucite window through which it views the simulated meteor; the product of these quantities is zero for $\lambda < 3400$ Å and $\lambda > 5800$ Å. Finally let $S_{\lambda o}$ be the absolute sensitivity (coulombs $joule^{-1}$) of the main PMT at a specific wavelength λ_o within its response range. Then

$$E'_{pg} = \frac{Q}{S_{\lambda o}} \int_{3300}^{5200} f(\lambda)P(\lambda)d\lambda \Big/ \int_{3400}^{5800} f(\lambda)g(\lambda)h(\lambda)d\lambda \quad . \qquad (3)$$

Laboratory calibrations of the PMT and of the lucite window, using a McPherson monochromator and an Eppley standard lamp with a radiant emittance calibration traceable to NBS standards, provided values for $S_{\lambda o}$, $g(\lambda)$, and $h(\lambda)$. Combining these with $f(\lambda)$ from Figures 2 and 3, our evaluation of (3) gave

$$E'_{pg}(Si) = 1.37 \times 10^{-5}\ Q \text{ joules} \qquad (4a)$$

and

$$E'_{pg}(Al) = 1.28 \times 10^{-5}\ Q \text{ joules} \quad . \qquad (4b)$$

But E'_{pg} is the radiant energy collected by the PMT, whereas what we desired was of course E_{pg}, the radiant energy emitted by the meteor.

The relation between these is

$$E_{pg} = N\, E'_{pg} \quad , \tag{5}$$

in which N is a dimensionless multiplying factor that depends upon the geometry of the experiment and the time variation of the instantaneous meteor intensity I_{pg}. If we assume the meteor to be an isotropic radiator and if we take Ω as the solid angle subtended by the PMT at the instantaneous position of the ablating particle,

$$N = 4\pi \int_0^\infty I_{pg}\, dt \Big/ \int_0^\infty I_{pg}\Omega\, dt \quad . \tag{6}$$

We might have utilized the same method as Becker and Friichtenicht to compute N, but two features of the experiment suggested an alternative approach. The first of these was the observation that N varied rather slowly with changes in the parameters of individual meteors due to the fact that the PMT's were located close to the position of maximum trail intensity; if extremes of short and long luminous trail lengths were excluded, the range of variation of N from one simulated meteor to another was no more than about ±10 percent. This implied that high precision was not necessary in the computation of N for any one event. The second feature was our decision, noted earlier, to make the anode time constant of the auxiliary PMT short enough that this tube responded to relative collected intensity ($I_{pg}\Omega$) instead of energy. Becker and Friichtenicht had developed a computer program for evaluation of N which was based upon a modification of (1) to give I_{pg} as a function of dm/dx, the mass loss per unit distance along the meteor trajectory, and on solutions of the meteor decay and heat transfer equations for dm/dx as a function of v and v as a function of x. In order to take advantage of the two features mentioned above, we modified that program so that it provided a series of curves (each corresponding to different combinations of such parameters as initial velocity, target gas pressure, etc.) of $I_{pg}\Omega$ versus x and a value of N for each curve. These curves corresponded to hypothetical outputs from the auxiliary PMT. For each datum we examined the auxiliary

PMT output signal as shown on the oscillogram, matched it as closely as possible to one of the computed curves, and then assigned to the datum the value of N associated with the selected curve. As determined in this manner, N varied from 1.39×10^3 to 1.71×10^3 for all acceptable events (i.e., those for which the peak intensity occurred when the ablating particle was between 14.7 cm and 23.0 cm from the target chamber entrance).

III. RESULTS AND DISCUSSION

After an initial screening to remove invalid events (principally cases of failure to meet our criterion for the spatial location of the point of maximum trail intensity), there remained the following numbers of acceptable data points: 108 for silicon particles in an air target gas (reduced to 104 in a second screening) with $13.0 \leq v_0 \leq 47.7$ km sec^{-1}; 33 for silicon in nitrogen with $21.1 < v_0 \leq 49.2$ km sec^{-1}; 22 for silicon in oxygen with $20.2 \leq v_0 \leq 45.8$ km sec^{-1}; 117 for aluminum in air (reduced to 106 in a second screening) with $12.0 \leq v_0 \leq 41.6$ km sec^{-1}; 19 for aluminum in nitrogen with $20.6 \leq v_0 \leq 43.3$ km sec^{-1}; and 25 for aluminum in oxygen with $20.0 \leq v_0 \leq 42.7$ km sec^{-1}. All results to be discussed are based upon these events, the data for all of which were reduced to τ_{pg} as described above.

The silicon-air and aluminum-air data were each averaged in 2 km sec^{-1} intervals of initial velocity (12.0-13.9 km sec^{-1}, 14.0-15.9 km sec^{-1}, etc.). The average values of τ_{pg}(Si) and τ_{pg}(Al) are plotted as functions of v_0 in Figures 4 and 5 respectively. In each figure the error bars extend $\pm\sigma$ except as noted and the smooth curves shown are visually-estimated best fits. Values of τ_{pg} obtained from the smooth curves are listed in Table 1.

The behavior of τ_{pg} for both materials with variations in velocity is qualitatively similar to that observed for iron and copper by Becker and Friichtenicht[3]: τ_{pg} first increases with increasing velocity but then peaks and declines as the velocity is increased further. In the case of silicon, τ_{pg} rises to a peak value of 1.77×10^{-3} (or 3.5×10^{-13} sec erg^{-1}, 0 mag) at 24 km sec^{-1} and then decays to 1.49×10^{-3} (3.0×10^{-13} sec erg^{-1}, 0 mag) at 30 km sec^{-1}, to 1.07×10^{-3} (2.1×10^{-13} sec erg^{-1}, 0 mag) at 40 km sec^{-1}, and to 0.79×10^{-3} (1.6×10^{-13} sec erg^{-1}, 0 mag) at the limit of our measurement, 48 km sec^{-1}. In the case of aluminum, τ_{pg}

TABLE 1

VALUES OF τ_{pg} FOR SILICON AND ALUMINUM MICROMETEORS*

Velocity (km sec^{-1})	Luminous Efficiency τ_{pg}			
	Silicon		Aluminum	
	(physical)	(sec erg^{-1}, 0 mag)	(physical)	(sec erg^{-1}, 0 mag)
12	---	---	0.00127	2.5×10^{-13}
14	0.00077	1.5×10^{-13}	0.00162	3.2×10^{-13}
16	0.00115	2.3×10^{-13}	0.00192	3.8×10^{-13}
18	0.00142	2.8×10^{-13}	0.00216	4.3×10^{-13}
20	0.00160	3.2×10^{-13}	0.00234	4.7×10^{-13}
22	0.00172	3.4×10^{-13}	0.00241	4.8×10^{-13}
24	0.00177	3.5×10^{-13}	0.00234	4.7×10^{-13}
26	0.00171	3.4×10^{-13}	0.00228	4.6×10^{-13}
28	0.00159	3.2×10^{-13}	0.00222	4.4×10^{-13}
30	0.00149	3.0×10^{-13}	0.00218	4.4×10^{-13}
32	0.00139	2.8×10^{-13}	0.00212	4.3×10^{-13}
34	0.00131	2.6×10^{-13}	0.00208	4.2×10^{-13}
36	0.00123	2.5×10^{-13}	0.00203	4.1×10^{-13}
38	0.00115	2.3×10^{-13}	0.00199	4.0×10^{-13}
40	0.00107	2.1×10^{-13}	0.00195	3.9×10^{-13}
42	0.00099	2.0×10^{-13}	0.00192	3.8×10^{-13}
44	0.00092	1.8×10^{-13}		
46	0.00086	1.7×10^{-13}		
48	0.00079	1.6×10^{-13}		

*Data taken from smooth curves, Figures 4 and 5.

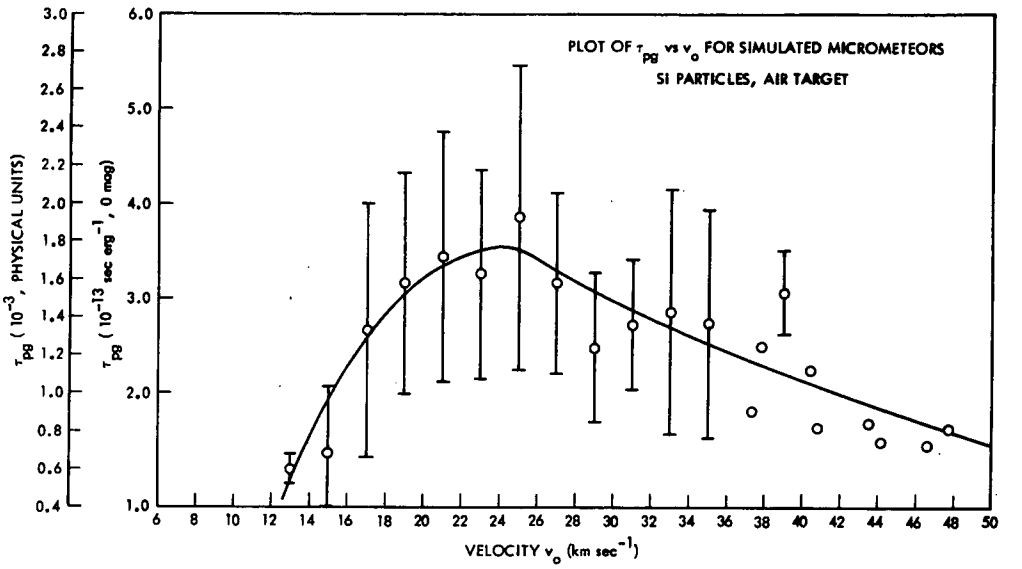

FIG. 4.--Plot of τ_{pg} for Si in physical and zero-magnitude units as a function of v_o. Data for each 2 km sec^{-1} interval have been averaged; error bars extend $\pm\sigma$. Points without error bars each represent a single datum.

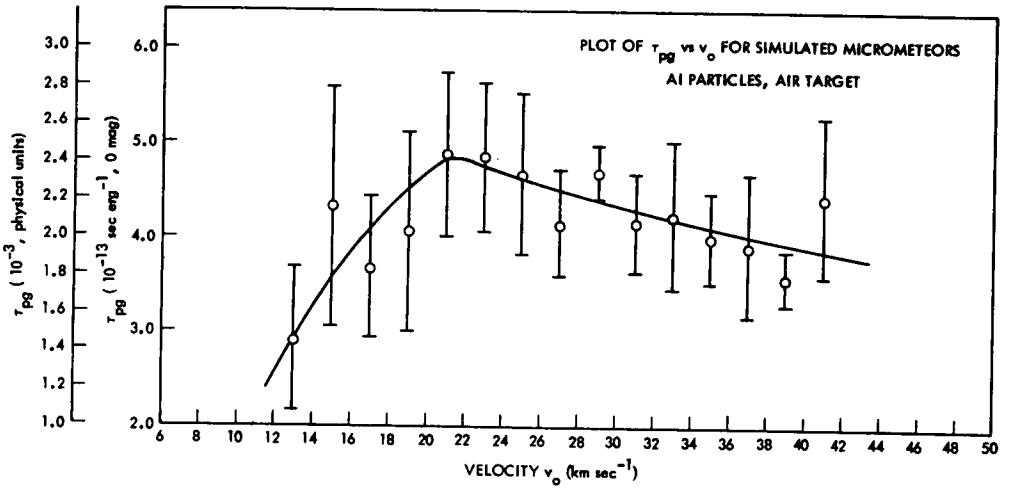

FIG.5.--Plot of τ_{pg} for Al as a function of v_o. Data averaging and error bar conventions are the same as in Fig. 4.

peaks at 2.42×10^{-3} (4.8×10^{-13} sec erg^{-1}, 0 mag) at 21 km sec^{-1}, declining to 2.18×10^{-3} (4.4×10^{-13} sec erg^{-1}, 0 mag) at 30 km sec^{-1} and to 1.92×10^{-3} (3.8×10^{-13} sec erg^{-1}, 0 mag) at the 42 km sec^{-1} limiting velocity of this measurement. Both τ_{pg}(Si) and τ_{pg}(Al) reach a peak at higher velocities than τ_{pg}(Fe), 18 km sec^{-1}, and τ_{pg}(Cu), 13.5 km sec^{-1}. The magnitudes of τ_{pg}(Si) and τ_{pg}(Al) are roughly comparable, although the former declines with increasing velocity rather more rapidly than the latter. The luminous efficiencies of both silicon and aluminum are lower than that of iron by factors of (roughly) 3-6 over the range $25 \leq v_o \leq 40$ km sec^{-1}; on the other hand, they are larger than τ_{pg}(Cu) in the same velocity range by about a factor of 4.

Data for particles ablating in pure nitrogen and pure oxygen were acquired as a check on the air results and the internal consistency of the experimental procedures; this is why we did not record as many events with these gases as with air. In Table 2, we list average values of τ_{pg}(Si) and τ_{pg}(Al) for the velocity intervals $20 \leq v_o \leq 29.9$ km sec^{-1}, $30 \leq v_o \leq 39.9$ km sec^{-1}, and $v_o > 20$ km sec^{-1}, and for nitrogen, oxygen, and air target gases. (The listed probable errors are $\pm\sigma$ of the averages.) Also tabulated are τ_{pg}(Si) and τ_{pg}(Al) computed for an air atmosphere from the sum of the nitrogen and oxygen values weighted by the relative abundances of the gases. Excellent agreement can be noted between the measured and calculated values of τ_{pg}(Al) in air at all velocity regimes. Good agreement is also found with silicon, particularly in view of the fact that greater scatter in the data for this material has resulted in a lower precision of measurement. (It may be noted at this time that since our experimental procedures were very similar to those of Becker and Friichtenicht, we feel that their estimate of the overall τ_{pg} measurement accuracy, ±40 percent, applies, along with their discussion of the nature and source of errors, to the current work as well.)

Figure 6 is a compendium of the following evaluations of photographic luminous efficiency of elemental meteoroid constituents: (a) Becker and Friichtenicht's measurement of τ_{pg}(Fe), supplemented at very low velocities ($v_o \approx 10$ km sec^{-1}) by τ_{pg}(Fe) data obtained for artificial iron meters by Ayers, McCrosky, and Shao[13]; (b) values of τ_{pg}(Mg) and τ_{pg}(Ca) determined by Boitnott and Savage[4,5]; (c) the current measurements of τ_{pg}(Si) and τ_{pg}(Al). (The only other experimental determinations of elemental luminous

TABLE 2

AVERAGE PHOTOGRAPHIC LUMINOUS EFFICIENCY $\langle \tau_{pg} \rangle_{av}$ FOR SILICON AND ALUMINUM MICROMETEORS IN VARIOUS ATMOSPHERES

Particle Material	Target Gas	$\langle \tau_{pg} \rangle_{av}$, Physical Units x 10^{-3}		
		20-29.9 km sec^{-1}	30-39.9 km sec^{-1}	>20 km sec^{-1}
Si	N_2	1.69 ± .56	1.02 ± .61	1.29 ± .68
	O_2	.64 ± .10	.62 ± .21	.62 ± .27
	air, calc.*	1.47	.94	1.10
	air, meas.	1.61 ± .59	1.40 ± .44	1.46 ± .56
Al	N_2	2.26 ± .30	2.09 ± .43	2.17 ± .39
	O_2	1.84 ± .25	1.36 ± .21	1.64 ± .31
	air, calc.*	2.17	1.94	2.06
	air, meas.	2.32 ± .40	1.98 ± .29	2.14 ± .39

*Calculated from $\langle \tau_{pg} \rangle_{av,air} = 0.79 \langle \tau_{pg} \rangle_{av,N_2} + 0.21 \langle \tau_{pg} \rangle_{av,O_2}$.

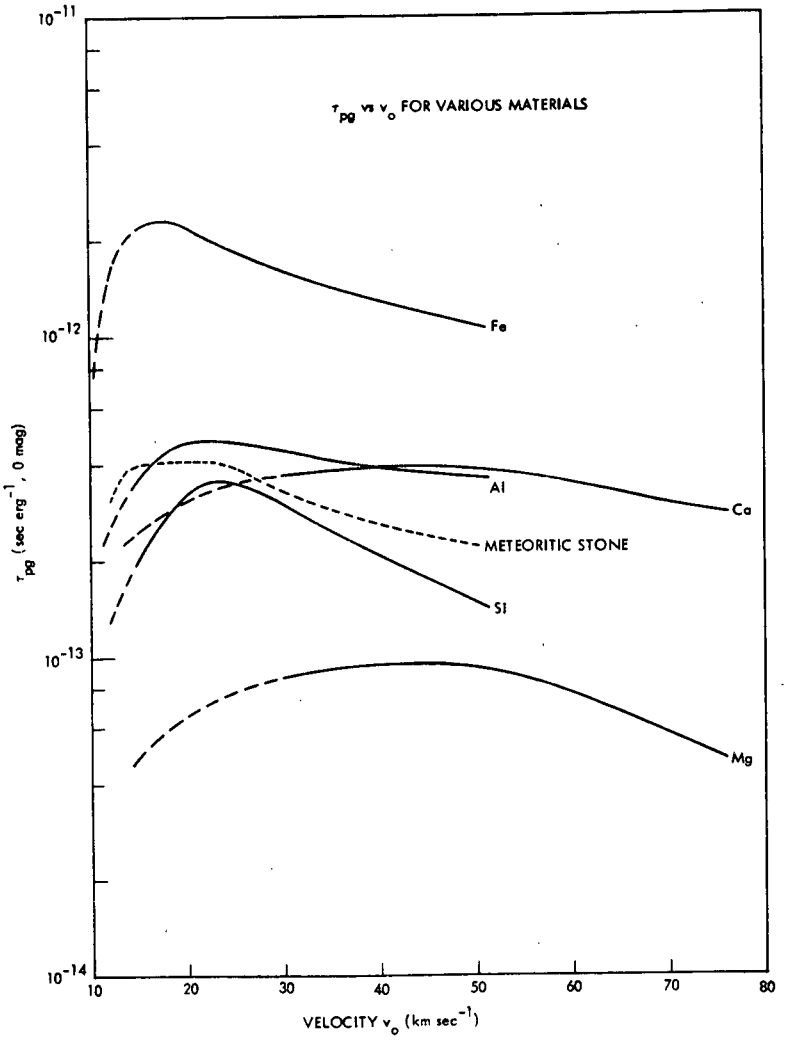

FIG. 6.--Plot of τ_{pg} as a function of atmospheric entry velocity v_o for meteoritic stone and for elemental constituents thereof. Data for τ_{pg}(Fe) are from Becker and Friichtenicht (Ref. 3); those for τ_{pg}(Mg) and τ_{pg}(Ca) are from Boitnott and Savage (Ref. 4, 1971); and those for τ_{pg}(Si) and τ_{pg}(Al) are from the current experiment. Results for meteoritic stone were computed from the elemental values using Eq. (7) in the text with relative mass abundances given by Öpik (Ref. 14).

efficiencies of which we are aware are those for copper by Becker and Friichtenicht, for sodium by Boitnott and Savage[4], and for potassium by Neff[6]; the latter two were omitted from the figure because neither sodium nor potassium radiates significantly within the limits of the blue-sensitive photographic spectrum, and the former was left out because copper is not known to be a constituent of naturally-occuring meteoroids.) There are several interesting features and relationships in the figure that should be mentioned. First of all, the notion that the photographic luminous efficiencies of at least some meteor constituents vary inversely with velocity--a notion first suggested, to our knowledge, by the theoretical work of Öpik[14] and first supported experimentally by Friichtenicht, Slattery, and Tagliaferri[2]--has now been confirmed, not only by our own results for silicon and aluminum but also by results for magnesium and calcium obtained by an entirely different experimental technique. Also of note is the trend toward smaller peak velocities for τ_{pg} with increasing atomic mass of the constituents. (The data for τ_{pg}(Cu), which show a peak at 13.5 km sec^{-1}, support this trend as well.) To be sure, departures from the trend are present: the broad peak of τ_{pg}(Ca) apparently occurs at 40-50 km sec^{-1}, greater than the peak velocities of τ_{pg}(Si) and τ_{pg}(Fe) even though the atomic mass of calcium is nearly midway between those of silicon and iron, and τ_{pg}(Al) appears to peak at a slightly lower velocity than τ_{pg}(Si) even though silicon is slightly heavier. We therefore hesitate to suggest that the trend is in fact a law. But as a trend subject to the possibility of an occasional exception it seems to be fairly firmly established, especially considering that the peak velocity relationship of τ_{pg}(Al) and τ_{pg}(Si) could be an artifact; given that the peak velocities differ by only 2 km sec^{-1} (<10 percent) in an experiment with an estimated ±40 percent limit of overall accuracy, the chance that the difference is actually in the opposite direction cannot be ruled out. On the other hand, we do not feel that a correlation between atomic mass and magnitude of τ_{pg} can be inferred from Figure 6 despite superficial appearances; such a correlation is contradicted by the Becker-Friichtenicht τ_{pg}(Cu) data and by the silicon-aluminum relationship, where in both cases the deviations from an assumed proportionality to mass are greater than the probable errors of the experiment.

An important point in their paper was Becker and Friichtenicht's

contention that the luminous efficiency $\tau_{pg}(M)$ of a meteor can be written

$$\tau_{pg}(M) = \Sigma_k A_k \tau_{pg}(k) \quad , \tag{7}$$

in which $\tau_{pg}(k)$ is the elemental luminous efficiency of a constituent k, A_k is the relative mass abundance of k, and the sum is over all constituents which are excited and which radiate within the photographic spectrum. Values for the relative abundances of elements in meteoritic stone have been given by Öpik[15], and Figure 6 contains all of the relevant values of $\tau_{pg}(k)$. (The only constituents mentioned by Öpik that are not included in the figure are sodium and potassium, whose spectral lines--as noted previously--lie outside the photographic spectrum; sulfur, emission from which does not appear significant in published meteor spectra[7]; and oxygen, which must be omitted because radiation from meteor-constituent oxygen is indistinguishable from that originating in collisionally-excited atmospheric oxygen.) Hence $\tau_{pg}(M)$ can be synthesized from (7), with the result shown by the dashed curve in Figure 6. This curve is roughly proportional to v^{-1} for $25 \leq v_o \leq 50$ km sec^{-1}, and except for a broader maximum its behavior is quite similar to that of iron. Such a result is hardly surprising, since the figure shows that $\tau_{pg}(Fe)$ greatly exceeds the luminous efficiencies of the other constituents over the entire range of velocities for which comparative measurements have been made and since the relative abundance of iron in meteoritic stone is high.

When Becker and Friichtenicht discovered that both $\tau_{pg}(Fe)$ and $\tau_{pg}(Cu)$ decreased with increasing meteor velocity, they were properly reluctant to draw inferences therefrom for the velocity dependence of $\tau_{pg}(M)$. Instead, they pointed out that the luminous efficiencies of other elements might increase at higher velocities and that the net result might then still be $\tau_{pg} = \tau_{op} v$, where τ_{op} is a constant, as determined by Verniani in his 1965 paper[1]. Now, however, the experimental results summarized above may correctly be said to have seriously weakened the $\tau_{op} v$ hypothesis, although it would be premature to regard that hypothesis as definitely falsified: There remain a number of uncertainties in our synthesis of $\tau_{pg}(M)$, not the least of which is the fact that Öpik's relative abundance data are based largely on analyses of meteorites and may require modification

for meteoroids prior to atmospheric entry. Nevertheless, it must be admitted that if τ_{pg} is proportional to v over a reasonable velocity range, then it should be possible to find some constituent or combination of constituents exhibiting similar behavior; it is hard to dismiss the fact that at least three separate groups of experimentalists employing at least two different experimental methods have so far failed to do so. A crucial experiment in this context would be the measurement of τ_{pg}(Mg) using the simulated meteor technique described herein. Such an experiment appears possible given the properties of the material and the limitations of the method of particle acceleration. If its findings should turn out to agree with those of Boitnott and Savage, then the validity of both kinds of experiment would have received a very strong confirmation and the hypothesis of proportionality to v would, we feel, be almost impossible to maintain.

IV. CONCLUSIONS

Simulated meteor experiments as described herein appear to offer a direct and fairly simple method for evaluating the luminous efficiencies of certain elemental meteor constituents and can be employed with a number of materials for which the measurement of emission cross sections by atomic beam techniques is not yet feasible. Through the use of submicron-sized particles, free molecule flow conditions are obtained at conveniently high target gas pressures. Occasional suggestions that the simulation is invalid due to the differences in absolute pressure between the experiment and the atmosphere remain conjectural; indeed, they are contradicted by the good agreement found by Becker and Friichtenicht between their measurement of τ_{pg}(Fe) at low velocities and that resulting from artificial meteors interacting with the real atmosphere.

Our measurements have given τ_{pg}(Si) and τ_{pg}(Al) for particles ablating in air over a velocity range 13-48 km sec^{-1} for silicon and 12-42 km sec^{-1} for aluminum. Although there do not now exist other data for τ_{pg}(Si) and τ_{pg}(Al) with which ours may be directly compared in the manner of the simulated and artificial meteor measurements of τ_{pg}(Fe), the following facts may be adduced in support of our results: (a) When τ_{pg} of silicon and aluminum in pure oxygen and pure nitrogen atmospheres were measured and the values used to compute an equivalent τ_{pg} for air, good agreement

with the measured values of τ_{pg} in air was observed for both materials. (b) The behavior of both τ_{pg}(Si) and τ_{pg}(Al) with increasing velocity resembles that found earlier for τ_{pg}(Fe) and τ_{pg}(Cu). (c) At least one feature--the velocity at which τ_{pg} reaches its peak value--varies more or less systematically from element to element. (d) Other researchers' evaluations of τ_{pg}(Mg) and τ_{pg}(Ca) based upon emission cross section measurements obtained by atomic beam methods exhibit behavior quite similar to those of our results, in terms of both order of magnitude and variation with velocity. A crucial confirming experiment could be the simulated meteor measurement of τ_{pg}(Mg), since this would permit a direct comparison with the atomic beam results.

Finally, our attempt to synthesize τ_{pg}(M) from the elemental constituent results, though admittedly subject to major uncertainties, appears to have cast some doubt upon the validity of the "law" $\tau_{pg}(M) = \tau_{op}v$. We are by no means prepared to offer our synthesis of τ_{pg}(M) as a positive replacement for the assumption of velocity proportionality; we do feel, however, that meteor photometric masses computed on the basis of that assumption should perhaps be considered more tentative than formerly believed until the question is positively resolved.

NOTES AND REFERENCES

1. For example, see: Z. Ceplecha and V. Padevět, Bull. Astr. Inst. Czechoslovakia, 12, 191 (1961); Z. Ceplecha, Bull. Astr. Inst. Czechoslovakia, 17, 347 (1966) and Smithsonian Ap. Obs. Spec. Rept., No. 279 (1968); F. Verniani, Smithsonian Contr. Ap., 8, 141 (1965) and Space Sci. Rev., 10, 230 (1970).

2. J. F. Friichtenicht, J. C. Slattery, and E. Tagliaferri, Ap. J., 151 747 (1968).

3. D. G. Becker and J. F. Friichtenicht, Ap. J., 166, 699 (1971).

4. C. A. Boitnott and H. F. Savage, Ap. J., 161, 351 (1970) and Ap. J. 167, 349 (1971).

5. H. F. Savage and C. A. Boitnott, Ap. J., 167, 341 (1971).

6. S. H. Neff, Ap. J., 173, 235 (1972).

7. P. M. Millman, Smithsonian Contr. Ap., 7, 119 (1963).

8. J. F. Friichtenicht, Rev. Sci. Instr., 33, 209 (1962).

9. H. Shelton, C. D. Hendricks, Jr., and R. F. Wuerker, J. Appl. Phys, 31, 1243 (1960); D. O. Hansen and N. L. Roy, Nucl. Instr. Methods, 40, 209 (1966).

10. N. L. Roy and D. G. Becker, Rev. Sci. Instr., 42, 204 (1971).

11. E. Tagliaferri and J. C. Slattery, Ap. J., 155, 1123 (1969).

12. C. W. Allen, Astrophysical Quantities (1st Ed; London: Athlone Press, 1955), p. 178.

13. W. G. Ayers, R. E. McCrosky, and C.-Y. Shao, Smithsonian Ap. Abs. Spec. Rept., No. 617 (1970).

14. E. J. Öpik, Physics of Meteor Flight in the Atmosphere (New York: Interscience Publishing Co., 1958), p. 139.

15. ibid.,p. 160.